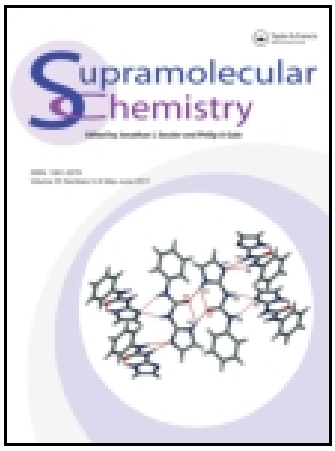

Supramolecular Chemistry
Publication details, including instructions for authors and subscription information:
http://www.tandfonline.com/loi/gsch20

Crystallographic, UV spectroscopic and computational studies of the inclusion complex of α-cyclodextrin with p-aminobenzoic acid

Kossay Elasaad [a b], Bernadette Norberg [a] & Johan Wouters [a]

[a] Department of Chemistry, University of Namur, rue de Bruxelles, 61, B-5000, Namur, Belgium

[b] Ministry of Higher Education in Syrian Arab Republic, 9251, Mezzeh Gamarik Square, Damascus, Syria

Published online: 03 Apr 2012.

To cite this article: Kossay Elasaad, Bernadette Norberg & Johan Wouters (2012) Crystallographic, UV spectroscopic and computational studies of the inclusion complex of α-cyclodextrin with p-aminobenzoic acid, Supramolecular Chemistry, 24:5, 312-324, DOI: 10.1080/10610278.2012.658392

To link to this article: http://dx.doi.org/10.1080/10610278.2012.658392

Supramolecular Chemistry
Vol. 24, No. 5, May 2012, 312–324

Crystallographic, UV spectroscopic and computational studies of the inclusion complex of α-cyclodextrin with *p*-aminobenzoic acid

Kossay Elasaad[a,b]*, Bernadette Norberg[a] and Johan Wouters[a]

[a]*Department of Chemistry, University of Namur, rue de Bruxelles, 61, B-5000 Namur, Belgium;* [b]*Ministry of Higher Education in Syrian Arab Republic, 9251, Mezzeh Gamarik Square, Damascus, Syria*

(*Received 17 October 2011; final version received 5 January 2012*)

Crystal structure of the cyclomaltohexaose (α-cyclodextrin, α-CD) inclusion complex with *p*-aminobenzoic acid (pABA) has been determined by X-ray diffraction. The host:guest stoichiometry is 1:1. The pABA molecule is included in the cavity with its axis coincident with the axis of α-CD; the benzoic group is inserted in the cavity, while the amino group sticks out from the cavity. Four water molecules are located near the cavity rims and in interstices between the molecules of α-CD participating in a dense network of intermolecular hydrogen bonds. UV–visible spectroscopy was applied to estimate the stability constant (K_c) at different temperatures on the basis of the Benesi–Hildebrand equation. This allowed calculation of complexation ΔH_c° and ΔS_c° on the basis of the Van't Hoff equation. The results are in good agreement with the values obtained by other methods in the literature. Phase-solubility profiles indicate that the solubility of pABA is significantly increased in the presence of α-CD at different pH values, and it was classified as A_L-type, indicating a 1:1 stoichiometric inclusion complex in solution. A theoretical investigation has also been carried out on the α-CD-pABA systems in order to search for other stable complexes. PM6 semi-empirical calculations were made to investigate equilibrium geometries of inclusion complexes formed between α-CD and neutral, anionic, cationic and zwitterionic forms of pABA. Two possible orientations were considered (A, with the carboxylic end inside the cavity and B, with the amino group inside the cavity). Preference between A and B orientations of each α-CD-pABA form results from different H-bond interaction patterns.

Keywords: cyclodextrin; *para*-aminobenzoic acid; crystal structure; inclusion complex; host–guest complex

1 Introduction

In pharmaceutical practice, poor water solubility of drugs is a well-known problem. At present, about 40% of the drugs in the development pipelines and up to 60% of the compounds coming directly from synthesis are poorly soluble (*1*). To act on target receptors, drugs must generally be dissolved in the physiological fluid and thereafter absorbed through entrance ports. Various methods have been used to increase the dissolution rate including micronisation, modification of the physico-chemical properties of the drug, addition of water-soluble polymers or complex formation with cyclodextrins (CDs).

Aminobenzoic acids are benzoic acid derivatives bearing an amino group in ortho, meta or para position of the aromatic ring. Among these structural isomers, only *p*-aminobenzoic acid (pABA) is of biological importance. pABA, known as vitamin H1, belongs to B-group vitamins. It is widely distributed in nature, participates in important biochemical processes (e.g. biosynthesis of folic acid) and reduces the mutagenicity of chemical mutagens (*2*). Moreover, pABA is used in the synthesis of some medicines (e.g. Novocain, 4-aminosalicylic acid) and as UV filter in sunscreen cosmetics (*3–5*). However, pABA can cause unwanted side effects, which can limit its industrial applications. For instance, dermatological side effects and pABA capability to damage DNA after UV irradiation were observed (*6–8*). To reduce these unwanted effects and to increase the aqueous solubility of the compound, the use of ABA forms encapsulated in CDs is an attractive goal.

Cyclomaltooligosaccharides (CDs) are cyclic oligosaccharides with α-$(1 \rightarrow 4)_n$-linked glucose units, where $n = 6$ (α-CD), $n = 7$ (β-CD) or $n = 8$ (γ-CD). CDs have a truncated conical structure (a torus) with the primary hydroxyl groups at the narrow side (head) and the secondary hydroxyl groups at the wide side (tail). CDs form inclusion complexes with a variety of molecules (*9*). Several factors are recognised to be responsible for the formation of inclusion complexes of CDs with suitable guest molecules: van der Waals forces and hydrogen bonds, as well as hydrophobic and dipole–dipole interactions (*10*). Crystal structures of α-CD complexes with various guests have been reported (*11*), suggesting that a para-substituted phenol is a suitable guest for α-CD. Crystal structures of α-CD complexes with *p*-hydroxybenzoic acid (*p*-$COOHC_6H_4OH$), *p*-nitrophenol (*p*-$NO_2C_6H_4$–OH), *p*-iodophenol and *p*-fluorophenol have been successfully determined (*12–14*). A number of studies were carried out

*Corresponding author. Email: kelasaad@fundp.ac.be

ISSN 1061-0278 print/ISSN 1029-0478 online

http://dx.doi.org/10.1080/10610278.2012.658392
http://www.tandfonline.com

on the inclusion complex of pABA with α-CD in solution using calorimetry, circular dichroism, fluorescence, ^{1}H NMR, fluorimetry and theoretical methods (*15–23*). To the best of our knowledge, no crystal structure of inclusion complex of pABA and α-CD has been reported so far.

In this study, the crystal structure of the α-CD and pABA inclusion complex has been determined, UV–visible spectroscopy has been applied to determine the stability constant (K_c) and thermodynamic parameters (ΔH_c° and ΔS_c°) of pABA complexation with α-CD and a theoretical investigation has been carried out on different α-CD-pABA systems in order to evaluate the relative stability of other stable complexes involving different forms of pABA.

2 Experimental

2.1 Materials

pABA (analytical reagent grade) and α-CD were purchased from Sigma-Aldrich (GmbH P.O. 1120, 89552 Steinheim, Germany). Other reagents were of analytical reagent grade and double distilled water was used throughout. Buffer solutions at pH = 1.5, 3.5 and 6.0 were prepared using phosphoric acid (85%) and its mono and disodium salts.

2.2 X-ray diffraction analysis

2.2.1 Crystallisation

Crystals of α-CD in complex with pABA were prepared by dissolving α-CD (0.1 mmol) in water (2.5 ml) at 65°C and pABA (0.1 mmol) in ethanol (2.5 ml) at 65°C. Both solutions were mixed and stirred at 65°C for 6 h. Then the mixture was stored at room temperature. Colourless crystals suitable for X-ray data collection were obtained by slow evaporation after 1 week.

2.2.2 X-ray diffraction experiment

X-ray diffraction experiment was carried out on an Oxford Gemini R Ultra using Mo K_α radiation ($\lambda = 0.71073$ Å) operating at 50 kV, 30 mA. A single crystal of the complex of α-CD-pABA was mounted on the head of the four-circle kappa goniometer. A total of 17,075 unique reflections were measured in the θ-range of 3.28–32.57°. Data reduction was carried out with the CrysAlisPro programme (*24*). Crystal data collection and refinement details are listed in Table 1. The structure belongs to the orthorhombic $P2_12_12_1$ space group with unit cell dimensions $a = 13.4823(3)$, $b = 15.5091(2)$ and $c = 24.8256(4)$ Å.

2.2.3 Structure solution and refinement

The structure of the complex was determined by direct methods and refined using full-matrix least-squares based on F^2 with the programme SHELX (*25*), based on 775 parameters and 2 restraints. The refinement converged to $R_1 = 0.0554$ for 9586 $F_0 > 4\sigma(F_0)$ and 0.1022 for all 17,075 data. Four water molecules (two ordered and two disordered

Table 1. Crystallographic data.

Chemical formula	$C_{36}H_{60}O_{36}.C_7H_7NO_2.4H_2O$
Formula weight (g mol^{-1})	1120.00
Temperature (K)	293(2)
Wavelength (Å)	0.71073
Crystal system	Orthorhombic
Space group	$P2_12_12_1$
a (Å)	13.4823(3)
b (Å)	15.5091(2)
c (Å)	24.8256(4)
A (°)	90.000
β (°)	90.000
γ (°)	90.000
Volume (Å^3)	5190.99(16)
Z	4
Crystal size (mm)	0.50 × 0.30 × 0.18
Calculated density (g cm^{-3})	1.498
Absorption coefficient (mm^{-1})	0.13
F(0 0 0)	2468
Theta range for data collection (°)	3.28–32.57
Limiting indices	$-20 \le h \le 17$, $-13 \le k \le 23$, $-37 \le l \le 33$
Reflections collected/unique	37,378/17,075
R (int)	0.0293
Data/restraints/parameters	17075/2/778
Goodness-of-fit (S) on F^2	0.9
Refinement method	Full-matrix least-squares on F^2
Final R indices (for 9586 with $F_0^2 > 4\sigma(F_0^2)$)	0.0553
Final R indices (all 17,075 data)	0.1021
Largest difference peak and hole (e/Å^3)	0.37 and −0.50

over two positions) were located in difference Fourier maps. All non-hydrogen atoms were anisotropically refined. Secondary hydroxyl groups were refined with two alternate conformations. Hydrogen atoms were calculated at ideal positions and refined using a riding model except those attached to some hydroxyl groups and on the two ordered water molecules that were located in difference Fourier maps.

2.2.4 Statistical search in the Cambridge structure database

A statistical survey of the Cambridge structural database (CSD) was performed searching for aromatic rings substituted by a carboxylic (—COOH), or carboxylate ($-COO^-$) group, and in its para position an amino ($-NH_2$), or ammonium ($-NH_3^+$) group. The statistical procedures used the VISTA software associated with CSD/2011 package (*11*). In this study, we focused on the C—O and C_{ar}–C bond lengths in carboxylic or carboxylate groups and on the C_{ar}–N bond length in amino or ammonium groups. The results were compared with the values in the crystal structure to establish the protonation state of pABA in the complex.

2.3 UV–visible absorption spectroscopy

UV–visible absorption spectra were recorded with a UVIKON XS spectrophotometer (Bio-TEK, Milano, Italy) at 1, 5, 10, 15, 20 and 25°C using 1 cm quartz cuvettes. Temperature was controlled by a cooling jacket Julabo bath circulation thermostat (model F30-HC/8 Julabo Labortechnik, Seelback, Germany) connected to the spectrophotometer. All solutions were prepared in distilled water. The concentration of pABA was held constant at 5×10^{-5} M. The concentration of α-CD varied from 0 to 5×10^{-3} M. The pH was controlled by 0.5 M phosphate buffers. Samples were incubated inside the spectrophotometer for 30 min at the working temperature before recording the spectra.

2.4 Phase-solubility diagram

Phase-solubility diagrams allow evaluation of the affinity between α-CD and pABA in water. Phase-solubility studies were carried out according to the method reported by Higuchi and Connors (*26*). pABA, in an amount that exceeded its solubility, was taken into a tube in which 10 ml of buffer (pH 6.0, 3.5 and 1.5) containing various concentrations of α-CD (0–25 mmol) was added. These tubes were sealed and shaken at 25°C for 72 h. This amount of time is considered sufficient to reach equilibrium. Subsequently, aliquots were filtered immediately through Whatman filter paper and diluted. A portion of the sample was analysed by UV spectrophotometer to determine the solubility of pABA by means of pABA calibration curves.

2.5 Computational methods

2.5.1 Ab initio geometry optimisation

Ab initio energy minimisation was performed on pABA in different ionisation forms (neutral/zwitterionic, protonated and deprotonated) to better approach geometry of the different protonation states. Calculation was done with the Gaussian09 (*27*) programme in the ground state using the 6-311G (5d, 7f) standard basis set and the B3LYP functional density method. Resulting geometries were compared with the crystal structure data retrieved from the CSD.

2.5.2 Semi-empirical simulation of complexes

Starting geometry for the α-CD-pABA inclusion complex was based on the crystal structure obtained in this work. In the first step, all water molecules were removed. Two possible orientations for pABA inside the α-CD cavity were simulated: in orientation A, the carboxylic group (COOH) of pABA is located inside the α-CD cavity while orientation B corresponds to the amino group (NH_2) inside the cavity (Figure 1). Orientation B was generated by exchanging the carboxylic and amino groups from the starting X-ray crystal structure by means of the builder module (Vega ZZ (*28*)). The final structures were saved as PDB file in order to prepare a suitable format file (OpenBabelGUI (*29*)) to start semi-empirical PM6 calculation (MOPAC2009 (*30*)). The input structures were edited to adjust the protonation state of pABA: cationic form (extra H on the amino group and charge $= +1$), anionic form (no H on the carboxylic group and charge $= -1$), neutral form (protonated carboxylic group and unprotonated amine, charge $= 0$) and zwitterionic form (unprotonated carboxylic group and protonated amine, charge $= 0$)). The systems were energy optimised using the PM6 method to locate low energy structures of complexes.

2.5.3 Effects of solvation on simulation of complexes

In order to study the influence of solvation on the overall stability of the complexes, all the previous starting structures (orientations A or B with the different protonation states for pABA) were placed in a 10 Å sphere containing 66 water molecules, and the same procedure of energy minimisation (PM6 level) was applied on those solvated systems.

3 Results and discussion

3.1 Crystal structure

The structures of the host and guest molecules are shown in Figure 2. Gn denotes the *n*th glucosidic residue of the α-CD. In our crystal structure, α-CD forms a 1:1 inclusion complex with pABA (Figure 3).

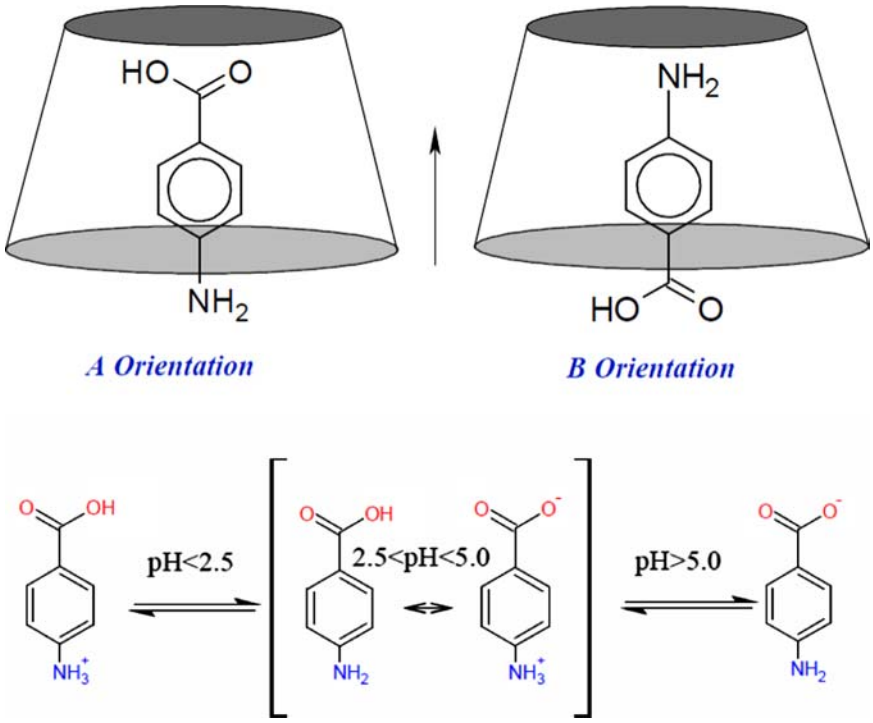

Figure 1. Two possible orientations of pABA (A and B) in α-CD (top), and pABA forms at different pH values (bottom).

3.1.1 *Geometry of the host molecule*

All glucose residues are in the normal $^4C_1$ chair conformation, and the overall α-CD molecules show distorted hexagon geometry. The diagonal distance measured between the glycosidic oxygen atoms (O_{4n}) is $O_{41}\cdots O_{44} = 8.289(2)$, $O_{42}\cdots O_{45} = 8.221(2)$, and $O_{43}\cdots O_{46} = 8.931(2)$ Å. A similar distorted structure was observed for other α-CD complexes with phenyl derivatives (*31*). Selected geometric parameters for the α-CD host molecule are listed in Table 2.

The glycosidic O_{4n} atoms lie in a plane within 0.0752 Å, the $O_{4n}\cdots O_{4(n+1)}$ distances varying between 4.103(2) and 4.468(2) Å, and the values of the angles between $O_{4(n-1)}\cdots O_{4n}\cdots O_{4(n+1)}$ differing significantly from 120°, the ideal value for an angle in a regular hexagon. Indeed, these values range from 113.71(4)° to 123.95(5)°, denoting that the cavity is distorted due to inclusion. The annular shape of α-CD is stabilised by inter-glucose hydrogen bonds connecting the secondary hydroxyl groups O_{3n} and $O_{2(n+1)}$ of the neighbouring glucosidic units (Table 2) (average $O_{3n}\cdots O_{2(n+1)}$ distance 2.849(2) Å, ranging from 2.708(2) to 2.984(2) Å). The orientation of the C_{6n}–O_{6n} bond is described by torsion angles C_{4n}–C_{5n}–C_{6n}–O_{6n} and O_{5n}–C_{5n}–C_{6n}–O_{6n}, listed in Table 2. Most of the primary hydroxyl groups (major disordered site) adopt the gauche–gauche conformation (mean torsion angles C_{4n}–C_{5n}–C_{6n}–O_{6n} and O_{5n}–C_{5n}–C_{6n}–O_{6n} 49.9(3)° and −71.4(3)°, respectively) and point out the cavity. In G3 and G5, O_{6n} is disordered in two sites with occupancy 60:40% in G3 and 75:25% in G5. A gauche-trans orientation is adopted for the second site and O_{6n} points inside the cavity. Four ordered water molecules are situated outside the cavity at the borders of the toroid rims and in interstices between α-CD molecules. Two water molecules, W2 and W4, are disordered in two sites with occupancy 50:50% and 60:40%, respectively. Table 3 lists the hydrogen bonds in this complex. No direct hydrogen bonds were found between the host and its guest.

3.1.2 *Geometry of the guest molecule*

In the crystal structure, the anionic form of pABA is observed in the inclusion complex with α-CD. Indeed, no extra electron density peak is observed in difference Fourier maps close neither to the COO^- nor to the NH_2 groups that could account for an extra H atom. Deprotonation of the carboxylic function is further established by similar values for the two C—O bond lengths (1.255(3) and 1.275(3) Å). The carboxylate and the benzene rings are coplanar with torsion angles: O_1–C_7–C_1–$C_2 = -0.1(5)°$, O_1–C_7–C_1–$C_6 = -178.4(3)°$, O_2–C_7–C_1–$C_2 = 177.2(3)°$ and O_2–C_7–C_1–$C_6 = -1.2(5)°$. Non-hydrogen atoms in pABA lie in a plane within 0.0343 Å, favouring electronic delocalisation and leading to a short C_{Ar}–C_7 distance equal to 1.473(4) Å. Delocalisation is prolonged to the nitrogen atom with a

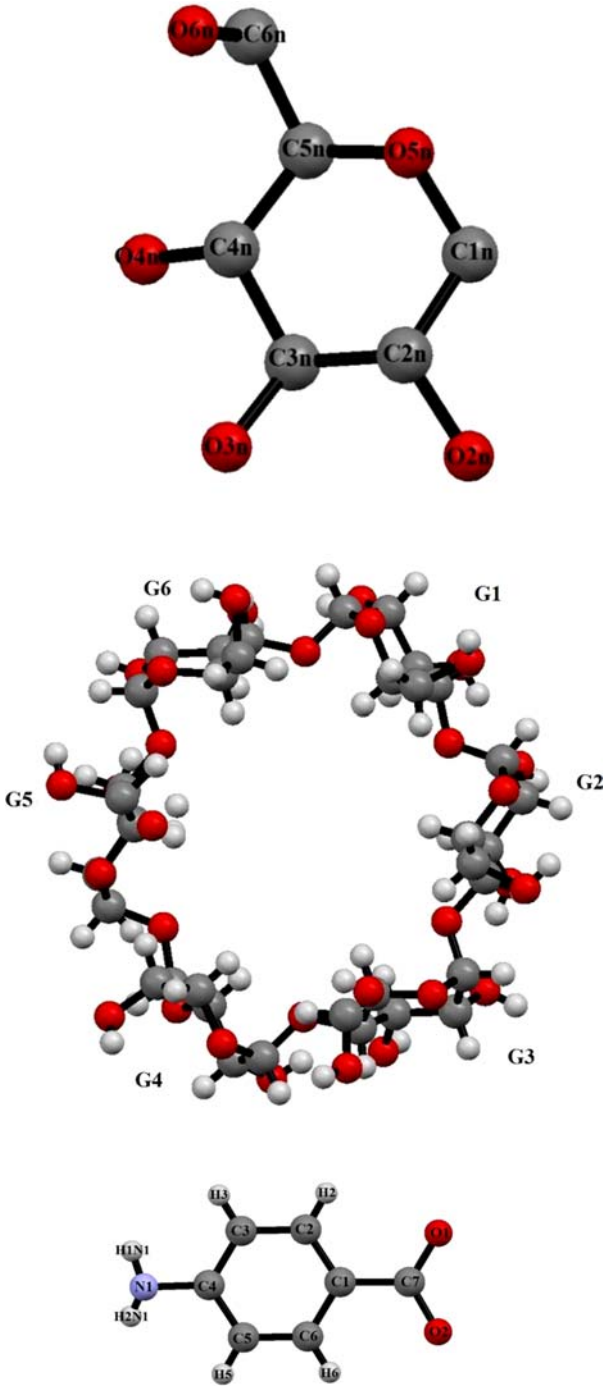

Figure 2. Structure and numbering scheme of α-CD and *p*-aminobenzoic acid. Only numbering of one glycosidic residue (Gn) of the α-CD is presented.

short C_{Ar}–N distance equal to 1.398(3) Å, and a marked sp^2 hybridisation character of the nitrogen atom with valence angles: C_4–N_1–H_{1N1} = 104.2(3.2)°, C_4–N_1–H_{2N1} = 108.7(3.7)° and H_{1N1}–N_1–H_{2N1} = 129.4(4.6)°.

A general search in the CSD (*11*) of aromatic compounds containing a carboxylic or amino group (see

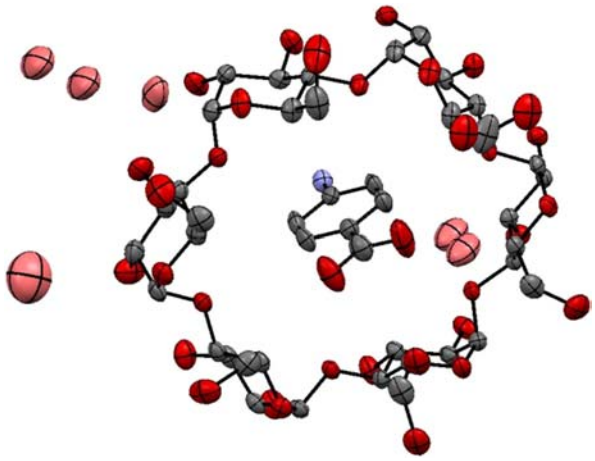

Figure 3. Axial view of the X-ray structure of the 1:1 host–guest inclusion complex of α-CD and pABA. Water molecules are shown with red light colour. Hydrogen atoms were omitted for clarity.

the supplementary data S1) confirms that the mean C—O bond lengths in Ar–COO^- fragments (1035 fragments retrieved) are 1.255(±0.022) and 1.253(±0.028) Å, and the mean of C_{Ar}–C_{carb} bond lengths is 1.509(±0.021) Å in case of the anionic forms (deprotonated). For Ar–COOH neutral forms (1259 fragments retrieved), the bonds differ significantly with C = O and C—OH mean bond lengths of 1.227(±0.025) and 1.302(±0.025) Å, respectively, and the mean of C_{Ar}–C_{carb} bond lengths is 1.485(±0.018) Å. The mean of C_{Ar}–N bond lengths in Ar–NH2 fragments (1696 fragments retrieved) is 1.396(±0.037) Å, and the mean of valence angles around N is C_{Ar}–N—H_1 = 115.1(±6.5)°, C_{Ar}–N—H_2 = 115.1(±6.2)° and H_1–N—H_2 = 115.3(±8.4)°. In Ar–NH_3^+ fragments (509 fragments retrieved), the mean of C_{Ar}–N bond length is 1.465(±0.014) Å, and the mean valence angles around N are C_{Ar}–N—H_1 = 110.157(±2.596)°, C_{Ar}–N—H_2 = 109.906(±3.195)°, C_{Ar}–N—H_3 = 110.0 (±2.6)°, H_1–N—H_2 = 108.8(±4.4)°, H_1–N—H_3 = 108.8 (±4.4)° and H_2–N—H_3 = 108.6(±5.8)°. The bond lengths in our crystal pABA molecule are 1.255(3) and 1.275(3) Å for C—O in carboxylic group, 1.395(3) Å for C_{Ar}–N and 1.472(4) Å for C_{Ar}–C, in good agreement with the values associated with an anionic form of pABA.

This is further confirmed by geometries optimised *ab initio* (B3LYP-6-311G (5d, 7f)) and with the semi-empirical PM6 method for the different protonation states of pABA: neutral, cationic, anionic and zwitterionic form (Table 4). According to the values coming from the theoretical studies and taking into account the experimental values, it is clear that the anionic form of pABA must be adopted in our crystal structure. This conclusion opens the question of the type and position of the counter cation. No extra electronic density was observed in difference Fourier maps that could correspond to a cation. So we suggest that

Table 2. α-CD macrocyclic characteristics.

Residue	$D_{O_4} - O_4$[a] (Å)	φ[b] (Å)	d[c] (Å)	$D_{O_3}\cdots O_2$[d] (Å)	Torsion angle (°) $C_{4n}-C_{5n}-C_{6n}-O_{6n}$	Torsion angle (°) $O_{5n}-C_{5n}-C_{6n}-O_{6n}$
G1	4.374 (2)	122.2 (1)	−0.098(1)	2.821(3)	42.9(3)	−78.6(3)
G2	4.194 (2)	123.9 (1)	0.050(1)	2.708(2)	49.7(3)	*70.5(3)
G3	4.105 (2)	113.7 (1)	0.056(1)	2.804(2)	51.5(12) 175.9(15)	−73.0(13) 59.7(23)
G4	4.468 (2)	122.8 (1)	−0.113(1)	2.985(2)	52.4 (2)	−69.9(3)
G5	4.171 (2)	122.3(1)	0.064(1)	2.883(3)	66.2(5)–153.3(17)	−55.0(4) 84.6(28)
G6	4.149 (2)	114.6 (1)	0.040(1)	2.883(3)	46.3(3)	−75.6(3)

[a] Distance between atoms $O_{4n}\cdots O_{4(n+1)}$.
[b] Angles between atoms $O_{4(n-1)}\cdots O_{4n}\cdots O_{4(n+1)}$.
[c] Deviations (Å) from the least-squares optimum plan of the six O_{4n} atoms.
[d] Intramolecular hydrogen-bond distance between $O_{3n}\cdots O_{2(n+1)}$.

one of the water molecules could be protonated to serve as a counter cation of anionic pABA.

3.1.3 Host–guest interaction

In the crystal structure, pABA is deeply inserted into the cavity of α-CD, with the amino group protruding from the wide side of the cavity and the carboxyl group at the narrow side as shown in Figure 3. The molecular plane of pABA forms an angle of 87.20(3)° with the plane made by the six O_{4n} atoms of the α-CD. The mass centre of the aromatic ring is 1.23 Å below the mass centre of the O_{4n} glycosidic atoms (see supplementary data S2). The corresponding values obtained from the β-CD-pABA inclusion complex are 72.3° and 1.64 Å (*23*). As a consequence, the pABA molecule better fits the α-CD cavity than the β-CD one, in

Table 3. Hydrogen bonds in α-CD–pABA complex with $H\cdots A < r(A) + 2.0$ Å and DHA > 110°.

D–H	A	d(D–H) Å	d(H..A) Å	<DHA°	d(D..A) Å
O21–H21O	O36	0.820	2.12	155.6	2.883(3)
O21–H21O	O46	0.820	2.30	113.8	2.740(3)
O22–H22O	O24 [$x-1/2, -y+1/2, -z$]	0.820	1.97	163.8	2.769(2)
O23–H23O	N1 [$x-1/2, -y+1/2, -z$]	0.820	1.95	167.8	2.755(3)
O24–H24O	O33	0.820	2.03	156.4	2.804(2)
O25–H25O	O34	0.820	2.19	164.8	2.985(2)
O25–H25O	O44	0.820	2.33	113.7	2.762(2)
O26–H26O	O4WA [$x+1, y, z$]	0.820	2.02	158.6	2.801(6)
O26–H26O	O4WB [$x+1, y, z$]	0.820	2.34	119.8	2.839(9)
O31–H31O	O22	0.820	2.00	174.6	2.821(3)
O32–H32O	O23	0.820	1.91	166.8	2.708(2)
O33–H33O	O35 [$x-1/2, -y+1/2, -z$]	0.820	2.03	133.6	2.666(2)
O34–H34O	O32 [$x+1/2, -y+1/2, -z$]	0.820	1.89	170.7	2.698(2)
O35–H35O	O26	0.820	2.11	157.0	2.885(3)
O36–H36O	O64 [$-x+3/2, -y+1, z+1/2$]	0.82	2.05	176.1	2.872(3)
O61–H61O	O33 [$-x+1/2, -y+1, z+1/2$]	0.820	2.14	125.4	2.701(3)
O62–H62O	O65A [$x-1, y, z$]	0.820	2.04	172.3	2.857(4)
O62–H62O	O4WB [$-x, y+1/2, -z+1/2$]	0.820	2.63	126.0	3.179(9)
O63A–H63A	O65A [$x-1/2, -y+3/2, -z$]	0.820	2.19	155.0	2.956(4)
O63B–H63B	O2WB	0.820	2.33	127.3	2.899(10)
O64–H64O	O36 [$-x+3/2, -y+1, z-1/2$]	0.820	2.30	127.7	2.872(3)
O65A–H65A	O1W [$x+1, y, z$]	0.820	2.07	166.5	2.872(4)
O65B–H65B	O21 [$-x+1, y+1/2, -z+1/2$]	0.820	2.52	144.2	3.220(9)
O66–H66O	O34 [$-x+3/2, -y+1, z+1/2$]	0.820	2.23	133.1	2.853(3)
N1–H1N1	O66 [$-x+1, y-1/2, -z+1/2$]	0.81(5)	2.21(5)	137(5)	2.861(3)
N1–H2N1	O25 [$x-1/2, -y+1/2, -z$]	0.95(5)	2.09(5)	171(5)	3.032(3)
O1W–H1W1	O52	0.856(19)	2.26(3)	157(5)	3.063(3)
O1W–H1W1	O65A [$x-1, y, z$]	0.856(19)	2.48(5)	109(4)	2.875(4)
O1W–H2W1	O4WB [$-x, y+1/2, -z+1/2$]	0.819(18)	2.28(5)	125(4)	2.837(10)
O3W–H1W3	O2 [$-x+1, y-1/2, -z+1/2$]	1.041(19)	1.73(4)	2.601(6)	138(5)
O3W–H1W3	O1 [$-x+1, y-1/2, -z+1/2$]	1.041(19)	2.50(3)	3.462(6)	152(4)
O3W–H2W3	O2WB [$-x+1, y-1/2, -z+1/2$]	1.024(19)	1.49(5)	2.248(9)	126(4)
O3W–H2W3	O2WA [$-x+1, y-1/2, -z+1/2$]	1.024(19)	1.70(3)	2.675(8)	158(5)

Notes: *A* refers to the first occupied site of disordered O_{6n}; *B* refers to the second occupied site of disordered O_{6n}.

Table 4. The bond lengths in carboxylic (or carboxylate) and amino (or ammonium) groups in different pABA forms resulting from *Ab initio* and PM6 minimisation.

		C_7–O_1 (Å)	C_7–O_2 (Å)	C_4–N_1 (Å)	C_1–C_7 (Å)
pABA (crystal structure)		1.2554 (31)	1.2753 (35)	1.3946 (33)	1.4725 (40)
Anionic-pABA	*Ab-initio*	1.280	1.280	1.410	1.530
	PM6	1.240	1.250	1.440	1.550
Neutral-pABA	*Ab-initio*	1.240	1.390	1.380	1.460
	PM6	1.210	1.390	1.390	1.460
Zwitterionic-pABA	*Ab-initio*	1.280	1.280	1.510	1.540
	PM6	1.230	1.230	1.500	1.560
Protonated-pABA	*Ab-initio*	1.230	1.370	1.510	1.490
	PM6	1.200	1.370	1.500	1.500

agreement with the results of studies in solution (*16*). It is noteworthy that the location of the aromatic ring is similar in other α-CDs complexes with aromatic guests (*12–14*, *34–37*). This is probably due to the fact that this position is sterically favourable for the aromatic ring.

Host–guest interactions play a crucial role in determining the orientation of guest molecules in the cavity of α-CD (*32*). In the case of the pABA-α-CD complex, the guest is held in the host cavity mainly by Van der Waals contacts (with α-CD) and hydrogen bonds (mediated through water molecules).

Selected observed hydrogen bonds in the complex are listed in Table 3. The bonds listed in the table are those for which the distance between the acceptor and the hydrogen atom is smaller than the radius of the acceptor atom plus 2.0 Å, and the angle between the donor atom, the hydrogen and the acceptor atom is larger than 110°.

No direct hydrogen bond is observed between α-CD and its included guest molecule. Indirect hydrogen bonds further stabilise pABA inside α-CD via water molecules. Additional hydrogen bonds involve the amino and carboxylic groups of pABA and the hydroxyl groups of adjacent α-CD molecules (see supplementary data S3 and Table 3).

3.1.4 Crystal packing

α-CD molecules are arranged in the crystal cell nearly parallel to its *ac* plane, forming a molecular layer (Figure 4). The least-squares plane through the six O_{4n} atoms forms an angle of 5.7° with respect to the *ac* plane. This crystal arrangement is different from the cage-type structure (*37–41*) since both ends of the cavity are open to the space between the layers. The α-CD molecules, which lie in the next layer, are slipped so that the overlap of the annular apertures is quite small. Therefore, in this arrangement, α-CD molecules do not form a continuous channel such as the one found in other channel type structures (*33*, *34*, *42*). The guest molecules are situated nearly parallel to the *bc* plane. The empty space between the α-CD molecules is filled with four water molecules. Crystal packing is further stabilised by intra-layers hydrogen bonds formed between hydroxyl groups, by the hydrogen bonds formed between the guests and hosts from different layers and by those formed between α-CDs molecules (see supplementary data S3).

3.2 UV-spectroscopy

Absorption spectra (between 200 and 350 nm) of pABA in the presence of increasing concentrations of α-CD are shown in Figure 5. In this wavelength range, pABA exhibits two maxima (284 and 222 nm) at pH = 3.5. The addition of increasing amounts of α-CD to the aqueous pABA solution resulted in a small bathochromic shift and a significant increase in the pABA absorption. These results confirm that pABA forms an inclusion complex with α-CD in solution. Inclusion of the pABA molecule into the macrocyclic cavity is accompanied by changes in its environment, causing changes in the absorption and a bathochromic shift.

In order to determine the stoichiometry and stability constant of the inclusion complex, the dependence of the pABA absorbance with respect to the α-CD concentration was analysed using the Benesi–Hildebrand Equation (*43*). Distinct equations are expected for a 1:1 (Equation (1)) or a 1:2 complex (Equation (2)) between pABA and α-CD.

$$A = A_0 + \frac{\Delta\varepsilon \cdot K_{(1:1)} \cdot C_{\mathrm{pABA}} \cdot [C_{\alpha-\mathrm{CD}}]}{1 + K_{(1:1)} \cdot C_{\mathrm{pABA}}}, \qquad (1)$$

$$A = A_0 + \frac{\Delta\varepsilon \cdot K_{(2:1)} \cdot C_{\mathrm{pABA}} \cdot [C_{\alpha-\mathrm{CD}}]^2}{1 + K_{(2:1)} \cdot C_{\mathrm{pABA}}}, \qquad (2)$$

where A and A_0 are the absorption of pABA in the presence and absence of α-CD, respectively; $\Delta\varepsilon = \varepsilon_{\mathrm{CD.pABA}} - \varepsilon_{\mathrm{pABA}}$ *is the difference in the molar absorptivities between free and complexed pABA;* C_{pABA} and $C_{\alpha\text{-CD}}$ are the initial concentrations of pABA and α-CD, respectively; K_c is the stability constant of the complex.

These equations can be rewritten in more useful forms (Equations (3) and (4)), which show a linear relationship between $(1/\Delta A)$ and $(1/(C_{\alpha-\mathrm{CD}}))$ in the case of a 1:1 complex.

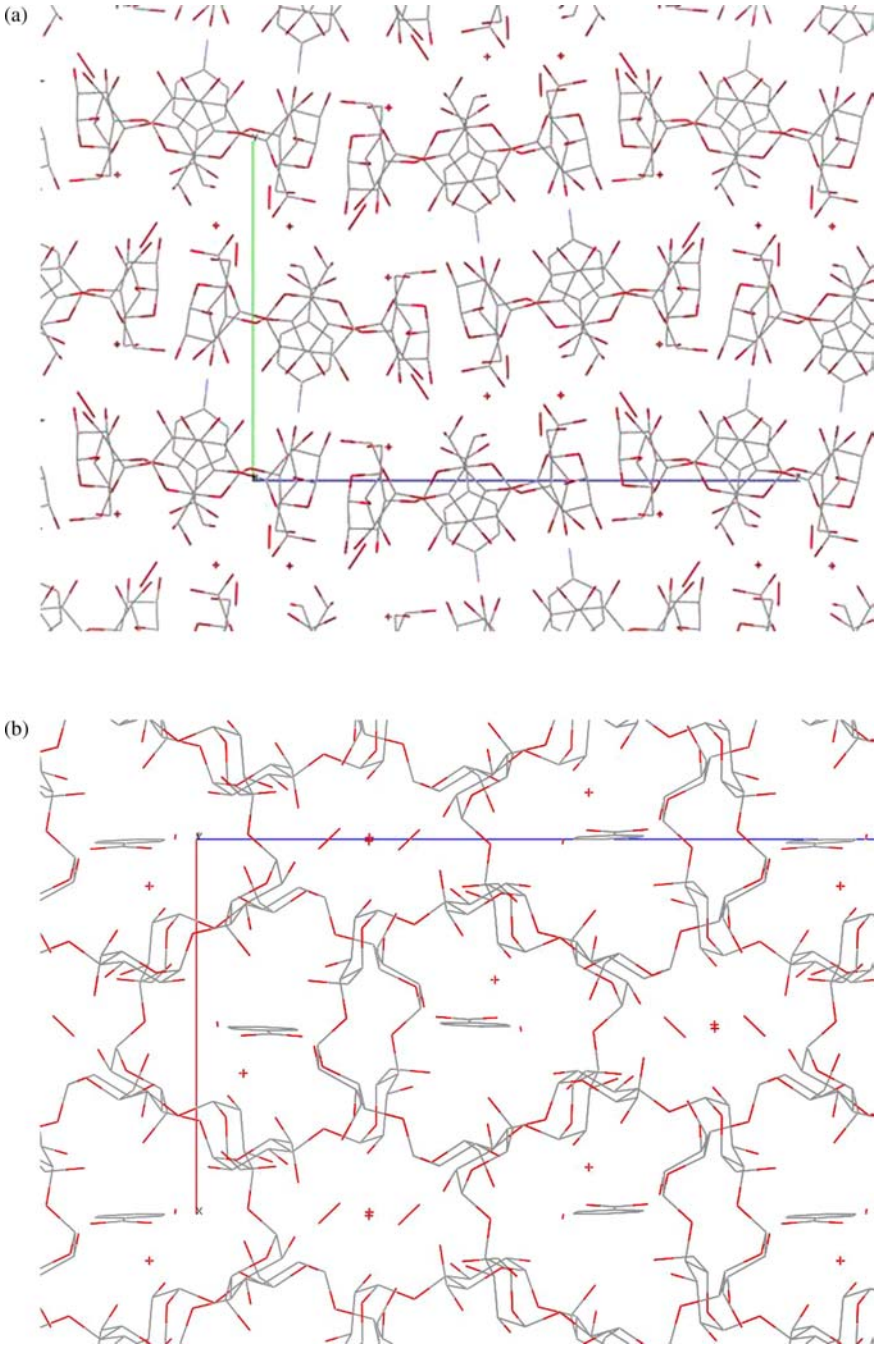

Figure 4. Drawing of the packing of the complex, viewed along *a*-axis (a) and *b*-axis (b).

$$\frac{1}{\Delta A} = \frac{1}{\Delta\varepsilon \times K_{(1:1)} \times C_{\text{pABA}}} \cdot \frac{1}{[C_{\alpha-\text{CD}}]} + \frac{1}{\Delta\varepsilon \times C_{pABA}}, \tag{3}$$

$$\frac{1}{\Delta A} = \frac{1}{\Delta\varepsilon \times K_{(2:1)} \times C_{\text{pABA}}} \cdot \frac{1}{[C_{\alpha-\text{CD}}]^2} + \frac{1}{\Delta\varepsilon \times C_{pABA}}. \tag{4}$$

In the case of pABA, the stability constants of the complex were determined by measuring the change in the maximum absorption of pABA (at ~280 and ~220 nm),

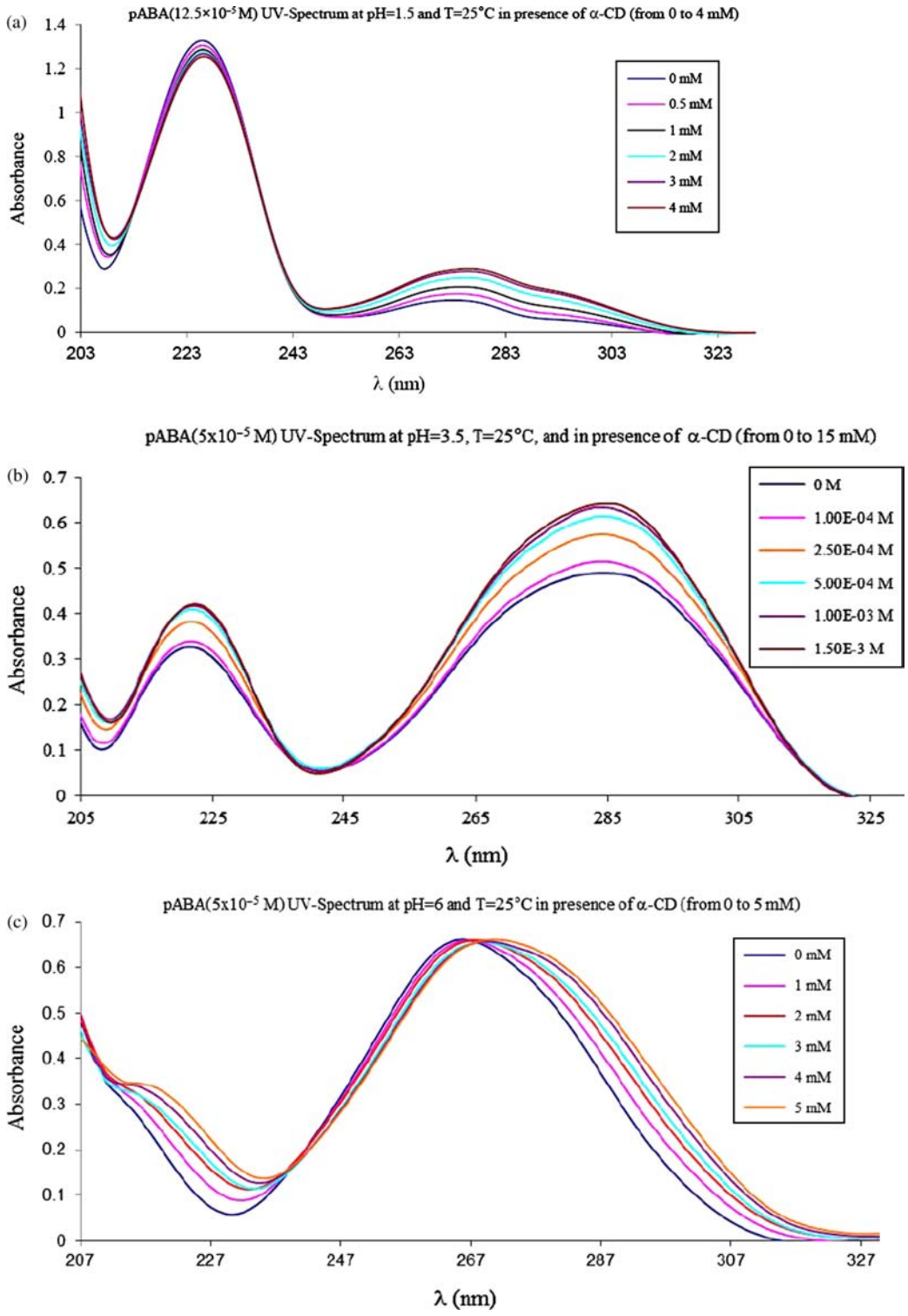

Figure 5. Absorption spectra of pABA: (a) 12.5×10^{-5} at pH = 1.5, (b) 5×10^{-5} M at pH = 3.5, (c) 5×10^{-5} M at pH = 6.0, in the absence and the presence of different concentrations of α-CD.

ΔA, in the presence of increasing concentrations of α-CD. The dependency of ΔA on the α-CD concentration is shown in Figure 6 (see also supplementary data S4). The data could be fitted to Equation (3) corresponding to a 1:1 stoichiometry. From these data, complexation constant, K_c, of pABA by α-CD is estimated to be 2319.4 ± 241.0 and 596.0 ± 80.5 M^{-1} at pH = 3.5 and 1.5, respectively, at $T = 25$°C. Values of 1400 ± 35 and 1000 ± 148 M^{-1}

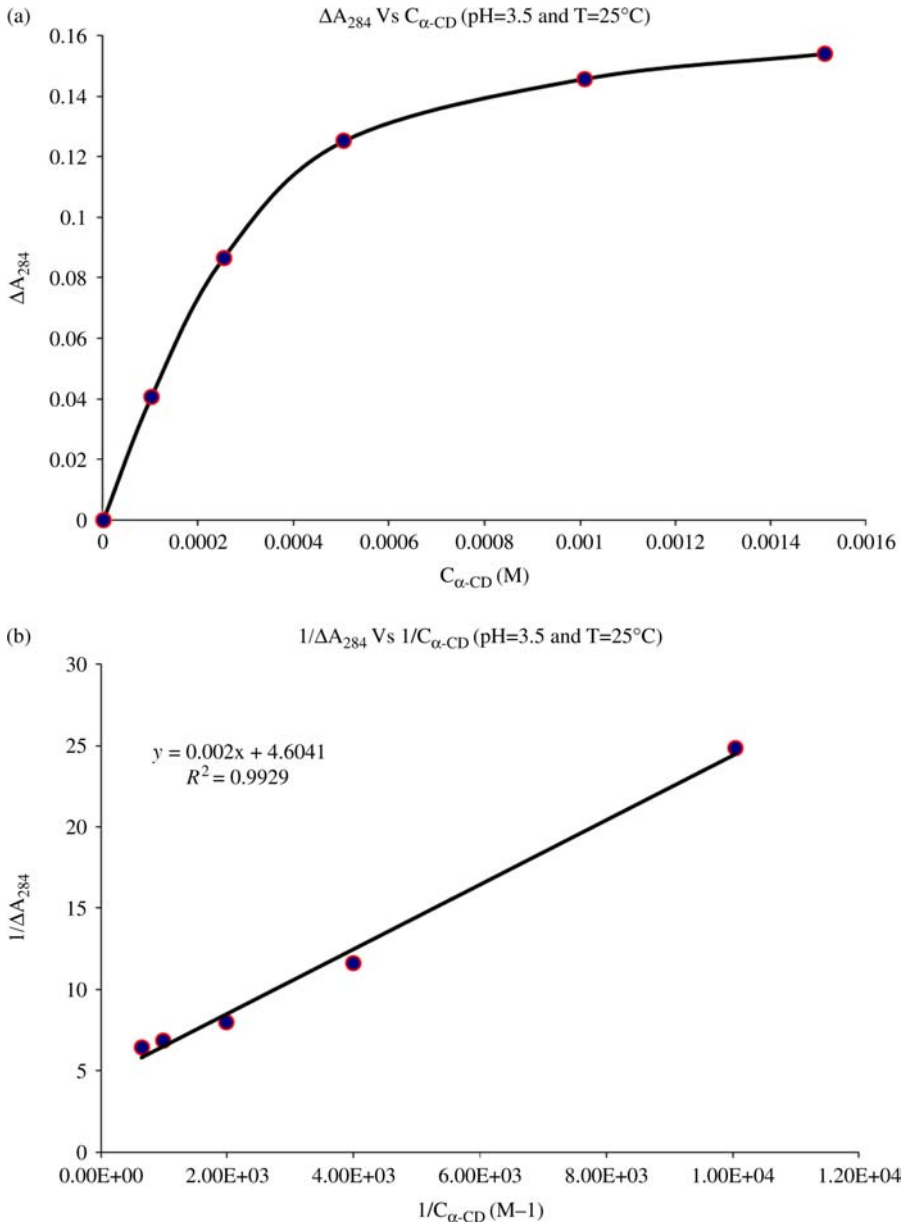

Figure 6. Dependence of ΔA_{max} of pABA solutions (5×10^{-5} M at pH = 3.5) on the α-CD concentration. Benesi–Hildebrand plots (linear relationship between $1/\Delta A$ and $1/C_{\alpha\text{-CD}}$) assuming formation of a 1:1 complex between pABA and α-CD give access to stability constants of the complex.

were obtained at pH = 3.5 and 2.0 ($T = 20$°C), respectively, by fluorescence method (*44*).

Repeating the same procedure at different temperatures (4, 10, 15, 20 and 25°C) showed that the stability constant increases with decreasing temperature (Table 5). The use of the Van't Hoff equation gives direct access to $\Delta H°$ and $\Delta S°$ of complex formation (Figure 7 and Table 6) (see also supplementary data S5). The data presented in Tables 5 and 6 indicate that the complex formation of pABA with α-CD is exothermic. Thus, the complex of pABA with α-CD is enthalpy–entropy stabilised. Enthalpy and entropy values include the contributions from the following main processes:

(1) partial breaking of the hydration shells of the solutes;
(2) exclusion of cavity-bound water molecules that are considered as 'enthalpy-rich' (*45*);
(3) conformational changes (e.g. deviation from symmetry and restriction of conformational flexibility);
(4) direct binding due to non-covalent interactions (van der Waals interactions, H-bonding, hydrophobic effects and electrostatic interactions) (*45*);
(5) hydration of complex.

The observed small $\Delta H°$ value (Table 6) may be a result of the important role of hydrophobic interactions

Table 5. Stability constants K (M^{-1}) for pABA-α-CD complex at pH = 3.5 and different temperatures.

	4°C	10°C	15°C	20°C	25°C
$K(\lambda_{max} = 222\,nm)\ M^{-1}$	3155.4 ± 298.3	2972.7 ± 317.3	2854.9 ± 317.5	2698.3 ± 314.6	2503.2 ± 272.2
$K(\lambda_{max} = 284\,nm)\ M^{-1}$	2880.2 ± 188.3	2686.1 ± 121.4	2505.2 ± 155.6	2414.7 ± 232.0	2319.4 ± 241.0

and dehydration of the solutes occurring upon penetration of the pABA molecule into the hydrophobic cavity of α-CD. This happens when the guest molecule is deeply inserted into the CD cavity, as can be seen from the crystal structure of the complex.

Positive entropy changes (Table 6) underline the extensive dehydration accompanied by the release of water molecules from the solvation shells of reagents into the bulk aqueous solution. Furthermore, hydrophobic interactions of the aromatic ring of pABA with the apolar cavity of CD can play a significant role in the complexation process, resulting in a positive $\Delta S°$ (*45*).

3.3 Phase-solubility diagrams

An apparent stability constant (K_c) can be calculated from the phase-solubility diagrams using Equation (5), according to the hypothesis of a 1:1 stoichiometric of the complex (*26*).

$$K_{(1:1)} = \frac{\text{slope}}{S_0(1 - \text{slope})}. \quad (5)$$

The slope was obtained from the initial straight line portion of the plot of the pABA solubility against the α-CD concentration, and S_0 is the equilibrium solubility of pABA in water.

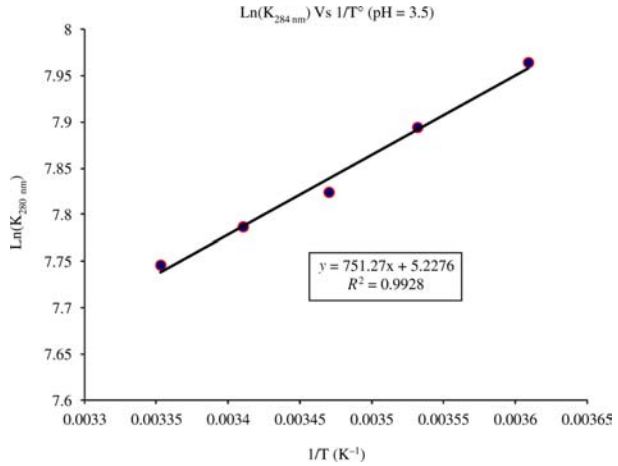

Figure 7. Van't Hoff analysis (dependence of Ln(K) of pABA-α-CD complex formation on the temperature ($1/T$) at pH = 3.5 (K values determined from data at $\lambda_{max} = 284$) give access to thermodynamic parameters $\Delta H°$ and $\Delta S°$ for the 1:1 complex formation of pABA with α-CD.

Phase-solubility diagrams for the complex formation between pABA and α-CD are presented (see also supplementary data S6). Our data indicate that the solubility of pABA in water depends on the pH of the solution: it is higher for the charged (protonated (pH = 1.5) and unprotonated (pH = 6)) forms: $S_0 = 0.145$, 0.030 and $0.170\,M^{-1}$ at pH = 1.5, 3.5 and 6.0, respectively. The phase-solubility diagrams show that the aqueous solubility of pABA increases linearly as a function of the α-CD concentration.

The linear host–guest correlation with a slope of < 1 confirms the formation of a 1:1 complex in solution with respect to α-CD concentration.

The increase in solubility of pABA resulting from inclusion in α-CD is more important at pH 3.5 (compare slopes). This study shows that the complex between pABA and α-CD is more stable at pH = 3.5, with an apparent stability constant, $K_{(1:1)}$, obtained from the slope of the solubility diagrams, of 736.9 ± 132.4 and 1710.7 ± $219.6\,M^{-1}$ at 25 and 4°C, respectively.

3.4 Semi-empirical simulation of complexes

pABA can exist in three forms (neutral, anion and cation) according to the pH of the environment (Figure 1). *Ab initio* (B3LYP-6-311G (5d,7f)) calculations have been applied to optimise the geometry of the different protonation forms of pABA alone. The results were used as a complement to crystal structures retrieved from the CSD to analyse the crystal structure of this guest in α-CD (see Section 3.1.2). Similar results have been obtained using the PM6 semi-empirical method. Based on those calculations, the most stable form is the protonated state ($E_{B3LYP} = -476.394$ A.U. (-12963.16 eV); $E_{PM6} = -1721.625$ eV) followed by the neutral and zwitterionic states ($E_{B3LYP} = -476.170$ (-12957.06 eV) and -476.064 A.U. (12954.18 eV); $E_{PM6} = -1715.149$ and -1712.645 eV, respectively). The anionic form is the less stable ($E_{B3LYP} = -475.604$ A.U. (12941.66 eV); $E_{PM6} = -1703.001$ eV). Interestingly, it is this last form

Table 6. $\Delta H°$ and $\Delta S°$ of complex formation, calculated from UV-spectroscopy data at pH = 3.5.

	$\lambda_{max} = 222$ nm	$\lambda_{max} = 284$ nm
$\Delta H°$ (kJ mol^{-1})	−8.69 ± 0.88	−6.25 ± 0.31
$\Delta S°$ (J K^{-1} mol^{-1})	35.9 ± 3.1	43.5 ± 1.1

that is observed in the crystal structure of the inclusion complex with α-CD, illustrating the fact that stabilisation effects resulting from complexation by the CD do affect differently the distinct protonation forms of pABA.

Therefore, different structures of α-CD-pABA inclusion complexes have been simulated. Two possible orientations of pABA inside the α-CD cavity have been retained, one (orientation A) with the carboxylic group of pABA located inside the α-CD cavity and the other (orientation B) corresponding to the amino group inside the cavity. For both orientations, the different protonation states of pABA (protonated, anionic, neutral or zwitterionic) were considered. The effect of solvation on the overall stability of the complexes was also approached. Energy minimisation of the different complexes was performed (PM6 level).

The optimised geometries were reasonable when water molecules were included in the calculation. In the absence of explicit water molecules, the *in vacuum* optimised complexes with neutral pABA (orientation A) or zwitterionic pABA (orientation B) converged to distorted geometries. This is in agreement with a similar study performed on inclusion complexes of pABA and β-CD (*46*). All the other systems converged to chemically reasonable complexes, suggesting that the PM6 method is well adapted to study the pABA-CD systems.

In particular, the PM6 method reproduced the crystal structure rather well. Indeed, the enthalpy of formation of pABA included in α-CD was the most negative with the anionic form of pABA, in orientation A ($H_{f(PM6)} = -4599.39$ kcal) compared to the anionic form of the guest in orientation B ($H_{f(PM6)} = -4583.40$ kcal). This result is in excellent agreement with the crystal structure reported in this study. The PM6 method suggests that complexation of the anionic form is favoured compared to the other protonation states of pABA ($H_{f(PM6)} = -4599.39$, -4519.80, -4481.46 and -4349.56 kcal) for complexes with anionic $pABA^-$, neutral pABA, zwitterionic $pABA^{+/-}$ and cationic $pABA^+$ forms, in orientation A. Similar calculations performed on complexes including pABA and β-CD (*46*) led to different results. In that work, orientation B was more stable but, in agreement with our results, the complex with anionic pABA was favoured.

The geometries of the studied complexes found with the PM6 method confirm that pABA is deeply included in α-CD, with the aromatic ring for each species of pABA totally embedded in the α-CD cavity especially for the A orientation.

4 Conclusions

Our crystallography study shows that pABA forms a 1:1 complex with α-CD and is deeply included into the cavity of the CD, with the amino group protruding from the wide side of the cavity and the (unprotonated) carboxylate at the narrow side. The crystal structure corresponds to the anionic form of pABA. The pABA guest is held in the host cavity mainly by Van der Waals contacts and hydrogen bonds. Spectroscopic studies of the interactions of pABA with α-CD demonstrate the insertion of pABA into the CD cavity in solution, with the formation of a 1:1 inclusion complex with stability constant $2319.4 \pm 241.0\,M^{-1}$ at 25°C and pH = 3.5.The phase-solubility studies confirm the formation of a 1:1 pABA-α-CD inclusion complex. The solubility of pABA in water is markedly enhanced by complexation with α-CD. The calculations carried out with the PM6 method show that inclusion complexes of different pABA protonation states with α-CD lead to stable structures and this confirms experimental observations. During this theoretical study, orientation A (carboxylic group inside) was more favourable than orientation B (amino group inside), in agreement with our crystal structure.

Supplementary data

Tables of atomic coordinates, bond lengths and bond angles have been deposited with the Cambridge Crystallographic Data Center, CCDC Nos. 845857 for the α-CD–pABA complex. These data may be obtained free of charge, on request, from The Director, Cambridge Crystallographic Data Center, 12 Union Road, Cambridge, CB2lEZ, UK (fax: +44-1223-336033; e-mail: deposit@ccdc.cam.ac.uk or http://www.ccdc.cam.ac.uk).

Additional data are available in the online supplementary information associated with this paper.

Acknowledgements

This study was supported by the Ministry of Higher Education in Syria in collaboration with chemistry biological structural laboratory (CBS), at the University of Namur (FUNDP) – Belgium.

References

(1) Merisko-Liversidge, E. Nanocrystals: Resolving Pharmaceutical Formulation Issues Associated with Poorly Water-Soluble Compounds., In Abstract of Papers, Particles Conference, Orlando, Florida, United States **2002**.
(2) Vasilieva, S. *Mutat. Res.* **2001**, *496*, 89–95.
(3) Hirt, R.; Hurni, H. *Helv. Chim. Acta* **1949**, *32*, 378–393.
(4) Bruze, M.; Gruvberger, B.; Thulin, I. *Photodermatol. Photoimmunol. Photomed.* **1990**, *7*, 106–108.
(5) Mackie, B.S.; Mackie, L.E. *Aust. J. Dermatol.* **1999**, *40*, 51–53.
(6) Salvador, A.; Chisvert, A.; Rodríguez, A.; March, J.G. *Anal. Chem. Acta.* **2003**, *493*, 233–239.

(7) Dromgoole, S.H.; Mailbach, H.I. *J. Am. Acad. Dermatol.* **1990**, *22*, 1068–1078.
(8) Shaw, A.A.; Wainschel, L.A.; Shetlar, M.D. *Photochem. Photobiol.* **1992**, *55*, 657–663.
(9) Bender, M.L.; Komiyama, M. *Cyclodextrin Chemistry*; Springer Verlag: Berlin, 1978.
(10) Malpezzi, L.; Fronza, G.; Fuganti, C.; Mele, A.; Brückner, S. *Carbohydr. Res.* **2004**, *339*, 2117–2125.
(11) Cambridge Structural Database System, Cambridge Crystallographic Data Centre 12 Union Road, Cambridge CB2 1EZ, UK. See http://www.ccdc.cam.ac.uk/products/csd/.
(12) Harata, K. *Bull. Chem. Soc. Jpn.* **1977**, *50*, 1416–1424.
(13) Harata, K. *Carbohydr. Res.* **1976**, *48*, 265–270.
(14) Harata, K. *Bioorg. Chem.* **1981**, *10*, 255–265.
(15) Lewis, E.A.; Hansen, L.D. *J. Chem. Soc. Perkin Trans.* **1973**, *2*, 2081–2085.
(16) Shuang, S.M.; Yang, Y.; Pan, J.H. *Anal. Chim. Acta.* **2002**, *458*, 305–310.
(17) Stalin, T.; Rajendiran, N. *Chem. Phys.* **2005**, *322*, 311–322.
(18) Stalin, T.; Shanthi, B.; Vasantha Rani, P.; Rajendiran, N. *J. Chem.* **2006**, *55*, 21–29.
(19) Stalin, T.; Rajendiran, N. *J. Photochem. Photobiol. A.* **2006**, *182*, 137–150.
(20) Terekhova, I.V.; Obukhova, N.A. *J. Solution. Chem.* **2007**, *36*, 1167–1176.
(21) Terekhova, I.V.; Kumeev, R.S.; Alper, G.A. *J. Incl. Phenom. Macrocycl. Chem.* **2007**, *59*, 301–306.
(22) Kartsova, L.A.; Komarova, N.V. *J. Analytical Chem.* **2003**, *58*, 972–978.
(23) Zhang, Y.; Yu, S.; Bao, F. *Carbohydr. Res.* **2008**, *343*, 2504–2508.
(24) CrysAlisPro, Oxford Diffraction Ltd.,Version 1.171.33.55. (Released on 05-01-2010 CrysAlis171.NET). See http://www.oxford-diffraction.com.
(25) Sheldrich, G.M. *Acta Cryst.* **2008**, *A64*, 112–122.
(26) Higuchi, T.; Connors, K.A. *Adv Anal chem. Instrum.* **1965**, *4*, 117–212.
(27) Gaussian 09; Revision A.02; Frisch, M.J.; Trucks, G.W.; Schlegel, H.B.; Scuseria, G.E.; Robb, M.A.; Cheeseman, J.R.; Scalmani, G.; Barone, V.; Mennucci, B.; Petersson, G.A.; Nakatsuji, H.; Caricato, M.; Li, X.; Hratchian, H.P.; Izmaylov, A.F.; Bloino, J.; Zheng, G.; Sonnenberg, J.L.; Hada, M.; Ehara, M.; Toyota, K.; Fukuda, R.; Hasegawa, J.; Ishida, M.; Nakajima, T.; Honda, Y.; Kitao, O.; Nakai, H.; Vreven, T.; Montgomery, Jr., J.A.; Peralta, J.E.; Ogliaro, F.; Bearpark, M.; Heyd, J.J.; Brothers, E.; Kudin, K.N.; Staroverov, V.N.; Kobayashi, R.; Normand, J.; Raghavachari, K.; Rendell, A.; Burant, J.C.; Iyengar, S.S.; Tomasi, J.; Cossi, M.; Rega, N.; Millam, J.M.; Klene, M.; Knox, J.E.; Cross, J.B.; Bakken, V.; Adamo, C.; Jaramillo, J.; Gomperts, R.; Stratmann, R.E.; Yazyev, O.; Austin, A.J.; Cammi, R.; Pomelli, C.; Ochterski, J.W.; Martin, R.L.; Morokuma, K.; Zakrzewski, V.G.; Voth, G.A.; Salvador, P.; Dannenberg, J.J.; Dapprich, S.; Daniels, A.D.; Farkas, O.; Foresman, J.B.; Ortiz, J.V.; Cioslowski, J.; Fox, D.J.; Gaussian, Inc. Wallingford, CT, See http://www.gaussian.com 2009.
(28) Vega ZZ release 2.3.2.38, Windows version., Copyright 1996–2009, Alessandro Pedretti & Giulio Vistoli. See http://www.vegazz.net.
(29) OpenBabelGUI © 2006 by Chris Morley, version 2.2.3 (released on 31-07-2009). See http://openbabel.org/wiki/Main_Page.
(30) MOPAC2009, James J.P. Stewart, Stewart Computational Chemistry, Version 9.310L. See http://OpenMOPAC.net.
(31) Harata, K. *Bull. Chem. Soc. Jpn.* **1977**, *50* (6), 1416–1424.
(32) Harata, K. *Chem. Rev.* **1998**, *98*, 1787–1802.
(33) Harata, K. *Bull. Chem. Soc. Jpn.* **1976**, *49*, 1493–1501.
(34) Harata, K. *Bull. Chem. Soc. Jpn.* **1976**, *49*, 2066–2072.
(35) Harata, K. *Bull. Chem. Soc. Jpn.* **1975**, *48*, 2409–2413.
(36) Saenger, W.; Beyer, K.; Manor, P.C. *Acta Crystallogr. Sect. B.* **1976**, *32*, 120–128.
(37) McMullan, R.K.; Saenger, W.; Fayos, J.; Mootz, D. *Carbohydr. Res.* **1973**, *31*, 211–227.
(38) Manor, P.C.; Saenger, W. *J. Am. Chem. Soc.* **1974**, *96*, 3630–3639.
(39) Saenger, W.; McMullan, R.K.; Fayos, J.; Mootz, D. *Acta Crystallogr. Sect. B* **1974**, *30*, 2019–2028.
(40) Saenger, W.; Noltemeyer, M. *Chem. Ber.* **1976**, *109*, 503–517.
(41) Hingerty, B.; Saenger, W. *J. Am. Chem. Soc.* **1976**, *98*, 3357–3365.
(42) Hybl, A.; Rundle, R.E.; Williams, D.E. *J. Am. Chem. Soc.* **1965**, *87*, 2779–2788.
(43) Benesi, H.A.; Hildebrand, J.H. *J. Am. Chem. Soc.* **1949**, *71*, 2703–2707.
(44) Shaomin, S.; Yu, Y.; Jinghao, P. *Analytica Chimica Acta.* **2002**, *458*, 305–310.
(45) Liu, L.; Guo, Q.-X. *J. Inclus. Phenom. Macrocycl. Chem.* **2002**, *42*, 1–14.
(46) Fatiha, M.; Djameleddine, K.; Leila, L. *Orbital* **2009**, *1* (1), 26–37.